J Ther Eng, Vol. 12, No. 1, pp. 99−114, January, 2026

Journal of Thermal Engineering
Web page info: https://jten.yildiz.edu.tr
DOI: 10.14744/thermal.0001061

Research Article

Numerical study of 3d thermal-flow in a scraped surface heat exchanger

Fatima Zohra BAKHTI[1,*], Belqassim Elmahdi ZERGUINE[2]

[1]*Department of Mechanical, Faculty of Technology, University Med Boudiaf, M'sila, 28000, Algeria*
[2]*Department of Mechanical, Faculty of Technology, University of Blida, Blida, 09000, Algeria*

ARTICLE INFO

Article history
Received: 24 October 2024
Revised: 17 March 2025
Accepted: 10 April 2025

Keywords:
CFD Modeling; Glycerin; Heat Exchanger; Heat Transfer Convection; Scraped Surfaces

ABSTRACT

This study investigates the thermal and fluid dynamics performance of scraped surface heat exchangers, optimizing key operational parameters to enhance heat transfer efficiency in processing viscous fluids. Using a numerical approach, the effects of blade count, rotational speed, and mass flow rate were analyzed. Results indicate that increasing blade count improves convective heat transfer, with a four-blade configuration enhancing the Nusselt number by 44.74% over a two-blade setup at 240 rpm. Higher rotational speeds reduce outlet temperatures by intensifying fluid mixing, though diminishing returns occur at very high speeds due to shorter residence times. These findings provide valuable insights for optimizing scraped surface heat exchanger design to balance thermal performance and energy efficiency, addressing critical needs in food, pharmaceutical, and chemical industries.

Cite this article as: Bakhti FZ, Zerguine BE. Numerical study of 3d thermal-flow in a scraped surface heat exchanger. J Ther Eng 2026;12(1):99−114.

INTRODUCTION

In the field of solar radiation utilization, solar thermal collectors are the most important parts of the solar thermal systems. However, the efficiency of these collectors is limited by the absorption properties of the working fluids, particularly water. Nanoparticle suspensions have been introduced as working media in solar thermal collectors to improve thermal efficiency and to reduce the size of such systems (energy efficient solar collectors) by using light induced energy conversion technique in a volume of suspended nanoparticles. It refers to direct absorption solar radiation (volumetric photo-thermal energy conversion), as shown in Figure 1. This figure shows the principles of photo-thermal energy conversion, where the incident solar radiation is directly absorbed by a volume of fluid which includes suspended particles. Then this energy is exploited in thermal applications. This method is one of the efficient methods in the field of energy conversion and production.

Scraped surface heat exchangers (SSHEs) are widely used across various industries to process high-viscosity substances. Their key advantage lies in efficiently handling such products, which would otherwise cause fouling and reduce heat transfer in traditional exchangers. SSHEs typically feature a rotor with blades that rotate inside a stationary stator, periodically scraping its inner surface to prevent fouling and maintain heat transfer efficiency. This scraping action also generates turbulence, further enhancing heat transfer.

*Corresponding author.
*E-mail address: fatimazohra.bakhti@univ-msila.dz

This paper was recommended for publication in revised form by Editor-in-Chief Ahmet Selim Dalkilic

SSHEs are used in various processes, including cooling, pasteurization, sterilization, crystallization, gelatinization, expansion, and texturing. They are particularly valuable in industries such as food, pharmaceuticals, chemicals, health, and beauty, where high-viscosity products are common. The performance of an SSHE depends on several factors like blade geometry, fluid flow rate, and fluid properties (viscosity, density, thermal conductivity, etc.). Therefore, careful design and optimization are essential for efficient heat transfer and mixing.

The surface scraping technique utilizes rotating blades or scrapers to continuously remove product build up or fouling from the heat transfer surface. This prevents deposit accumulation, maintaining a clean surface and enhancing heat transfer efficiency. This method is especially useful in industries where fouling or scaling is common, as it improves exchanger performance and reduces maintenance requirements.

Scraped surface heat exchangers (SSHEs) have been studied for decades, with early research dating back to Huggins [1] in 1931, who investigated the effects of mechanical scrapers on heating, cooling, and mixing performance. Since then, numerous advancements have been made in SSHE design and implementation.

Trommelen and Beek [2] analyzed flow phenomena in SSHEs, focusing on the Couette flow regime and Taylor vortices. Their findings demonstrated how these flow patterns influence heat transfer and identified specific operational regimes that maximize thermal efficiency. Harrod [3] conducted a comparative analysis of various SSHE designs, examining their impact on heat transfer efficiency. This study provided insights into SSHE flow patterns, mixing effects, residence time distribution, heat transfer performance, and power requirements. Lee and Singh [4] investigated the residence time distribution (RTD) of particle flow in a vertical SSHE, aiming to characterize particle movement under varying operational conditions. Their findings highlighted the influence of design parameters, such as scraper speed and flow rate, on particle retention and mixing efficiency.

De Goede and De Jong [5] investigated heat transfer properties in scraped surface heat exchangers (SSHEs) operating under turbulent flow conditions. Their study focused on key indicators, such as the convective heat transfer coefficient and temperature profiles, to enhance the understanding and optimization of SSHE thermal performance. Cenedese et al. [6] utilized Laser Doppler Anemometry (LDA) and Particle Image Velocimetry (PIV) to analyze velocity profiles and turbulent structures in fluid jets. Their research demonstrated the effectiveness of these methods in visualizing and analyzing complex flow dynamics. Baccar and Abid [7] conducted a numerical analysis of three-dimensional flow and thermal behavior in an SSHE under varying axial and rotational Reynolds numbers. Their results highlighted the impact of scraper geometry and motion on flow patterns and thermal efficiency.

Alhamdan and Sastry [8,9] investigated the effects of particle shape, concentration, and fluid viscosity on heat transfer in SSHEs. Their findings revealed that higher particle concentrations and irregular shapes increase fluid resistance, negatively impacting heat transfer dynamics. Additionally, higher viscosities were shown to reduce flow velocity and heat transfer rates. Baccar and Abid [10] conducted numerical simulations to analyze the hydrodynamic and thermal behavior of an SSHE under turbulent flow conditions. Their study examined the interaction between flow dynamics and heat transfer, emphasizing the role of scraper movement in turbulence generation and boundary layer disruption. Results demonstrated that scraper action significantly enhances convective heat transfer by improving mixing and reducing thermal resistance. Lakhdar et al. [11] studied the freezing process in SSHEs, focusing on the influence of flow rate, rotor speed, and blade clearance on heat transfer. Their findings highlighted the critical role of blade geometry in optimizing thermal performance during freezing operations. Yataghene et al. [12] used Particle Image Velocimetry (PIV) to analyze flow patterns in SSHEs under continuous flow. Their study identified complex fluid dynamics, including recirculation zones and secondary flows, influenced by blade geometry, rotational speed, and fluid properties. Yataghene and Legrand [13] conducted numerical simulations to investigate the coupled fluid flow and heat transfer of pure glycerin, a 2% CMC solution, and a 0.2% Carbopol solution inside an SSHE. They examined heat exchanger performance under varying blade speeds and mass flow rates, finding that increasing the rotating velocity optimized the average exit temperature.

Martínez et al. [14] investigated heat transfer during ice slurry production in scraped surface plate heat exchangers, focusing on the influence of phase change, scraper motion, flow conditions, and operating parameters on thermal performance. Using both experimental and numerical methods, they analyzed heat transfer coefficients and ice crystal formation dynamics. Dehkordi et al. [15] studied heat transfer in Surface Scraped Heat Exchangers (SSHEs), particularly for high-viscosity fluids prone to fouling. Their numerical analysis identified rotor speed as the most influential factor, with higher RPMs significantly enhancing heat transfer. Other key parameters include fluid flow rate, blade design, and heat flux mechanisms. Blasiak and Pietrowicz [16] conducted experimental studies on SSHEs under turbulent flow conditions, measuring heat flux (500–1500 W/m^2) and convective heat transfer coefficients (20–45 W/m^2K). They proposed an empirical correlation for the Nusselt number Nu= 1.765 Rer0.496.Pr0.33 to describe heat transfer in these exchangers. Martínez et al. [17,18] introduced a thermocouple-based technique for real-time wall temperature monitoring in SSHEs, enhancing thermal management and performance optimization, particularly for viscous fluids. Their analysis of flow patterns in a rotating scraped surface plate heat exchanger demonstrated the impact of rotation on fluid dynamics, leading to improved mixing and heat transfer efficiency.

The study conducted by Pordanjani et al. [19] investigated a Scraped Surface Heat Exchanger (SSHE) configuration that consists of an encased rotor with two blades mounted on it. The main focus of the research is to examine the impact of rotor speed and mass flow rate on the heat transfer efficiency of the SSHE and outlet temperature. This research also shows that decreasing the outgoing heat flux from the heat exchanger reduces the convection heat transfer coefficient.

Maruoka et al. [20] designed an SSHE with a rotating cylindrical tube and fixed blade to remove solid PCM layers during discharging. At rotational speeds up to 500 rpm, heat release rates increased six fold compared to stationary conditions, with 80% of latent heat extracted in 15 minutes versus only 50% in four hours without scraping. They achieved a maximum heat transfer coefficient of 2000 W/m^2K. Carlos et al. [21] examined the thermal behavior and phase transition of a non-Newtonian fluid in a dynamic SSHE under varying operating conditions. Using computational fluid dynamics (CFD) simulations validated by experiments, they analyzed the impact of scraper motion, fluid properties, and heat transfer dynamics on the glass transition process.

Tombrink & Bauer [22] and Tombrink et al. [23] investigated rotating drum heat exchangers for latent heat storage using both simulation and experimental methods. Their findings demonstrated that rotation enhances heat transfer, reduces thermal resistance, and ensures uniform temperature distribution, optimizing the melting and solidification of phase change materials (PCMs). Ding et al. [24] analyzed the heat and mass transfer performance of a Scraped Surface Heat Exchanger (SSHE) in suspension freeze concentration (SFC) processes. Through experimental and computational approaches, they examined heat transfer coefficients, mass transfer dynamics, and phase change behavior. The results highlight that scraper motion significantly improves fluid mixing, enhances heat and mass transfer, and minimizes fouling. Egea et al. [25] evaluated a novel SSHE for latent energy storage in domestic hot water systems. The device showed high thermal efficiency during phase change processes. The scraping action prevented PCM solidification, ensuring stable performance across multiple cycles. Solano et al. [26] studied heat transfer and pressure drop in reciprocating SSHE tubes, examining the impact of varying scraping amplitudes. Their findings indicate that greater scraping amplitudes enhance fluid mixing, disrupt thermal boundary layers, and improve convective heat transfer efficiency. Imran et al. [27] investigated the electro-osmosis-induced flow of a Jeffrey viscoelastic fluid in a Scraped Surface Heat Exchanger (SSHE). They analyzed the combined effects of electro-kinetic forces and the fluid's viscoelastic properties on heat and mass transport. Using mathematical modeling and computer simulations, they examined velocity profiles, temperature distributions, and pressure gradients under varying operational parameters, including electro-osmotic flow intensity and fluid elasticity. The results highlight the dual role of electro-osmosis in enhancing flow dynamics and improving thermal transfer efficiency. Egea et al. [28] examined a Scraped Surface Heat Exchanger (SSHE) for solar energy storage, with an emphasis on preventing the build-up of solid PCM layers. Their key findings include faster energy release at higher HTF flow rates, optimal temperature differences between 20–25°C, and the identification of a critical scraping frequency for improved efficiency. Additionally, they proposed a highly accurate predictive model for solidification time.

Allehiany et al. [29] analyzed heat transfer in scraped surface heat exchangers (SSHEs) using a Williamson fluid model with electroosmotic effects in a narrow-gap design. Computational methods (BVP4C in MATLAB) and analytical solutions explore velocity, temperature, and pressure profiles under varying parameters like Weissenberg and Brinkman numbers. Results show that viscoelastic behavior enhances fluid flow, while electro-osmosis and medium mobility impact temperature and velocity. These results are validated against artificial neural network (ANN) predictions. Rahman and Dhiman [30] investigated a novel perforated conical baffle plate design with air deflectors to improve heat transfer in tubular heat exchangers. This design enhances turbulence and increases thermal efficiency by 2.51 times compared to conventional baffles. The study identified key performance factors, including the deflector inclination angle and pitch ratio, which significantly impact friction.

Despite these advancements, significant gaps remain in understanding the complex flow patterns and heat transfer mechanisms within SSHEs, particularly under extreme operational conditions such as high rotational speeds or when handling non-Newtonian fluids. While previous studies have made substantial progress in modeling SSHEs, many are limited by simplified assumptions, such as constant fluid properties or the lack of detailed geometric modeling. These limitations hinder the development of more accurate predictive models that can capture the full range of thermal and fluid dynamics in SSHEs under realistic operating conditions. In addition, Experimental analysis of these systems is often limited by difficulties in measuring local variables like velocity and temperature in real time. As a result, there is an urgent need for a comprehensive numerical model capable of accurately capturing the intricate thermal and fluid dynamics of SSHEs under realistic operating conditions

This study aims to bridge these gaps by developing a comprehensive three-dimensional numerical model that integrates the complexities of real-world SSHE systems, including non-constant fluid properties, detailed blade configurations, and realistic operational conditions. By building on recent advancements and addressing the limitations in current models, this work seeks to provide more accurate insights into the thermal and fluid dynamics of SSHEs, particularly in applications involving high-viscosity Newtonian fluids. The findings will offer valuable guidelines for optimizing SSHE performance and improving their efficiency in industrial processes.

GENERAL DESCRIPTION OF SSHES

The studied configuration, as well as the boundary conditions, are presented in Figures 1 to 4. It is an outer Aluminum cylinder (stator) with length L and diameter Ds, in which the outer wall maintains constant temperature Tp= 278.16 K. Within this cylinder, blades with thickness e are attached to the stainless steel inner shaft cylinder (rotor) with diameter Dr rotating at a constant rotation speed ω=120 rpm, 240 rpm, 360 rpm, 480 rpm, 600 rpm, scraping exchange surface. The clearance between the blade tip and the exchange surface δ=130μm. All dimensions of the configuration considered in this work were exactly the same as those given by Yataghene et al. [12,13]; they are summarized in Table 1.

The working fluid is Glycerin, modelled as a Newtonian fluid in a laminar regime with a viscosity that depends on temperature. Table 2 gives the physical properties of pure Glycerin, Stainless steel, and Aluminum used in the calculations.

Table 1. Geometrical Characteristics of the SSHE [13,15]

Characteristic	Value
Stator diameter, D_s	0.065m
Rotor diameter, D_r	0.04m
Stator length, L	0.4m
Total surface heat exchange, S_{ex}	0.095m^2
Total volume, V_t	0.0015m^2
Blade-stator clearance, δ	130μm
Blade thickness, e	0.005m
Number of blades	2-3-4

Table 2. Physical properties of materials [13,15]

Material	Viscosity(Pa.s)	Thermal conductivity (W.m^{-1}.K^{-1})	Heat capacity (J.kg^{-1}.K^{-1})	Density (kg.m^{-3})
Pure Glycerin	$\mu_T = 8.1.10^{-12}.\exp\left(\frac{7378.8}{T}\right)$	0.285	2435	1240
Stainless steel	-	16.27	502.48	8030
Aluminum	-	202.4	871	2719

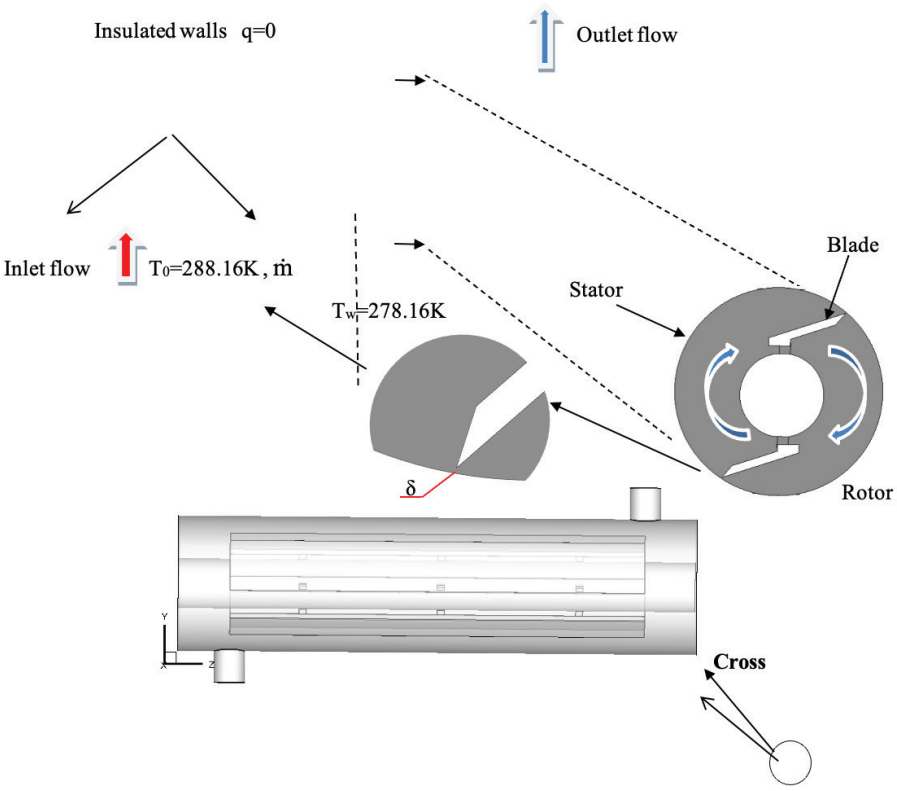

Figure 1. Computational domain and boundary conditions of SSHE, longitudinal and transversal cross-section.

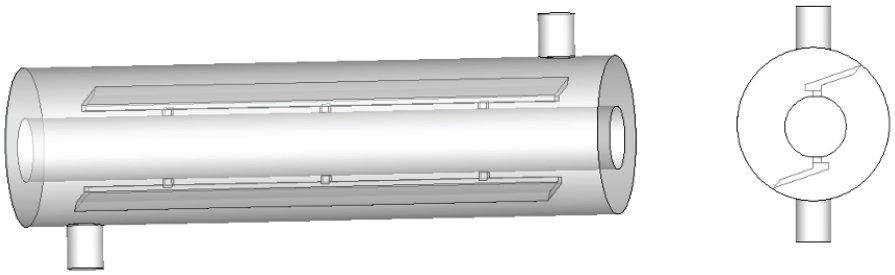

Figure 2. Isometric view of SSHE with 02 blades and transversal cross-section.

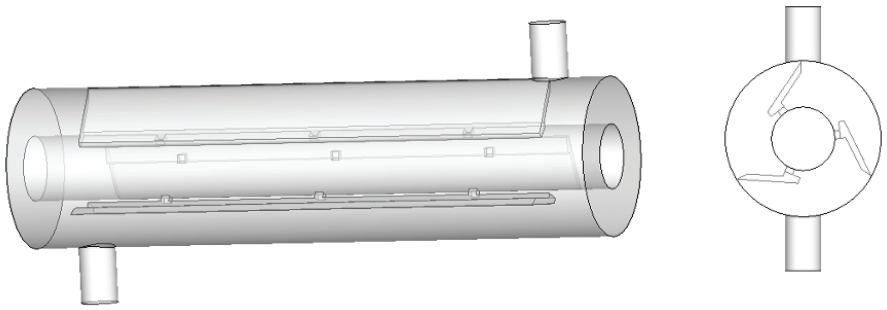

Figure 3. Isometric view of SSHE with 03 blades and transversal cross-section.

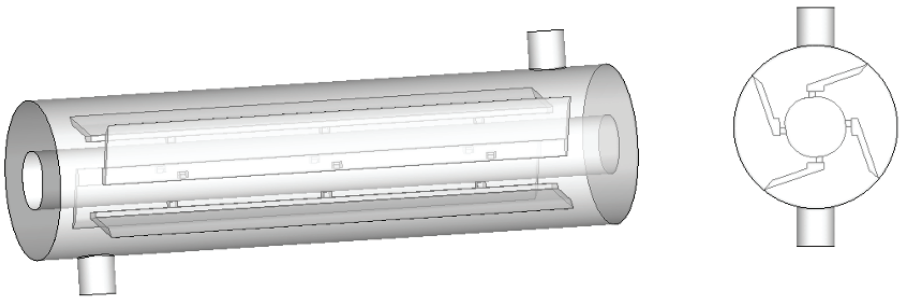

Figure 4. Isometric view of SSHE with 04 blades and transversal cross-section.

Governing Equations and Boundary Conditions

The fluid flow coupled with heat transfer within a scraped surface heat exchanger (SSHE) involves the consideration of non-isothermal, incompressible laminar flow. The conservation equations of mass, momentum, and energy are solved using Fluent software based on the Finite Volume Method. Due to the significant rotation of the fluid induced by the rotor and blades in the SSHE, it is essential to utilize the rotating reference frame formulation to address the continuity, momentum, and energy equations. The primary purpose of employing a moving reference frame is to transform an unsteady problem in the stationary (inertial) frame into a steady one relative to the moving frame [15]. When solving rotating frame problems with Fluent software, it is possible to use either the absolute velocity, $\vec{v}$, or the relative velocity, $\vec{v}_r$, as the dependent variable. These two velocities are related by an equation that allows for the accurately modelling of the fluid dynamics and heat transfer processes within the SSHE.

In steady-state conditions for the relative velocity, the system of equations can be written in the following vector form [12,13,15] :

The continuity equation

$$\nabla\left(\rho.\overrightarrow{V_r}\right) = 0 \tag{1}$$

$$\vec{V_r} = \vec{V} - (\vec{\omega}.\vec{r}) \tag{2}$$

Where,
$\vec{\omega}$ is angular velocity.
$\vec{V}$ is absolute velocity.
$\vec{r}$ is the position vector in rotating frame

-The momentum equation

$$\nabla\left(\rho\vec{V_r}.\vec{V_r}\right)+\rho\left(2\vec{\omega}.\vec{V_r}+\vec{\omega}.\vec{\omega}.\vec{r}\right)=-\nabla p+\nabla\bar{\bar{\tau}}_r+\rho.\vec{g} \quad (3)$$

$2\vec{\omega}.\vec{V}_r$ is the Coriolis acceleration
$\vec{\omega}.\vec{\omega}.\vec{r}$ is the centripetal acceleration

-The energy equation

$$\nabla\left(\rho.\vec{V_r}.H_r\right)=\nabla\left(k_f.\nabla T\right)+\nabla\left(\bar{\bar{\tau}}_r.\vec{V_r}\right) \quad (4)$$

The terms used in the equation (4) are forced heat convection, heat conduction, and viscous dissipation. The relative internal energy (Er) and relative total enthalpy (Hr) are the two terms used to express the energy equation. The following is a definition of these variables [34]:

$$E_r=h-\frac{p}{\rho}+\frac{1}{2}(V_r^2-(\omega.r)^2) \quad (5)$$

$$H_r=E_r+\frac{p}{\rho} \quad (6)$$

Boundary Conditions

As shown in Figure 1, the rotor and its blades, which are assumed to be thermally insulated, rotate at speeds ranging from 120 rpm to 600 rpm. The fluid enters the system at a temperature of 288.16 K with a mass flow rate between 0.017 kg/s and 0.086 kg/s and undergoes cooling. The heat transfer process involves passing the coolant over the stator to maintain a constant heat flux condition on the casing. The fluid flow adheres to the no-slip condition throughout the system, at solid surfaces and exits under both hydrodynamically and thermally fully developed conditions [12,13].

-At the stator surface: Tw=278.16K, v=0 (No-slip wall condition at the wall)

-On the rotor: insulated wall q=0, v=ω.r

-On the blades: insulated wall q=0, v=ω.r

-Inlet flow: mass flow rate ṁ , T_0=288.16K

-Outflow: $\left(\frac{\partial v}{\partial n}\right)=0$, $\left(\frac{\partial T}{\partial n}\right)=0$

-The average Nusselt number is calculated according to the following expression [31,32]:

$$\overline{Nu}=\frac{\bar{h}.d}{k_f}=\frac{q_c}{A.(\bar{T}_w-\bar{T}_m)}.\frac{d}{k_f} \quad (7)$$

Where $\overline{T}_w$ is the average temperature of the walls of the SSHE.

$\overline{T}_m$ is the average temperature of the fluid.

-The improvement of the heat transfer in the SSHE with 3 and 4 blades compared to the SSHE with two blades is estimated by percentage enhancement of the Nusselt number as follows [33,34]:

$$Enhancement\ \overline{Nu}_{3,4}\%=\frac{\overline{Nu}_{3,4}-\overline{Nu}_2}{\overline{Nu}_2}.100 \quad (8)$$

Where ;

$\overline{Nu}_{3,4}$ the average Nusselt number of SSHE with 3 and 4 blades.

$\overline{Nu}_2$ the average Nusselt number of SSHE with 2 blades.

NUMERICAL MODELING

Mesh Independence Study

For the three models of the scraped surface heat exchanger, tetrahedral cells were generated to mesh the computation domain as shown in Figure 5. A refined mesh is essential near places where there are high variations in flow properties, such as near the stator and the tips of blades, to capture the low fluid deformations.

In numerical studies, it is necessary to verify the effect of mesh resolution on the solution to ensure the accuracy and reliability of the numerical solution before performing calculations. Mesh independence was verified using different mesh sizes, as shown in Figure 6. The average convection coefficient ($\bar{h}$) was determined for all mesh faces at a mass flow rate ṁ = 0.017236 Kg/s and a rotational speed ω = 240 rpm. From Figure 6, we observe that the difference between the average convection coefficient values for the last three mesh sizes is slightly different, and the coefficient ($\bar{h}$) becomes insensitive to the number of nodes in the mesh at 876347. Therefore, we have chosen 876347 nodes for all our calculations to obtain accurate results with minimal computational time.

Number of nodes	$\bar{h}$(W/m².K
120797	287,62
178925	287,13
256341	286,81
314946	286,09
529173	285,82
619865	285,73
749532	285,61
876347	285,48
921875	285,43
987653	285,41

Solver Setting

Solidworks and Gambit software are used to create and mesh the geometry. Fluent6.3.26, a computational fluid dynamics (CFD) program, uses a finite volume approach to solve integral equations controlling mass, momentum, fluid conservation, and solid phase energy after receiving the mesh file. This model uses Fluent›s SIMPLE algorithm, a 3D double

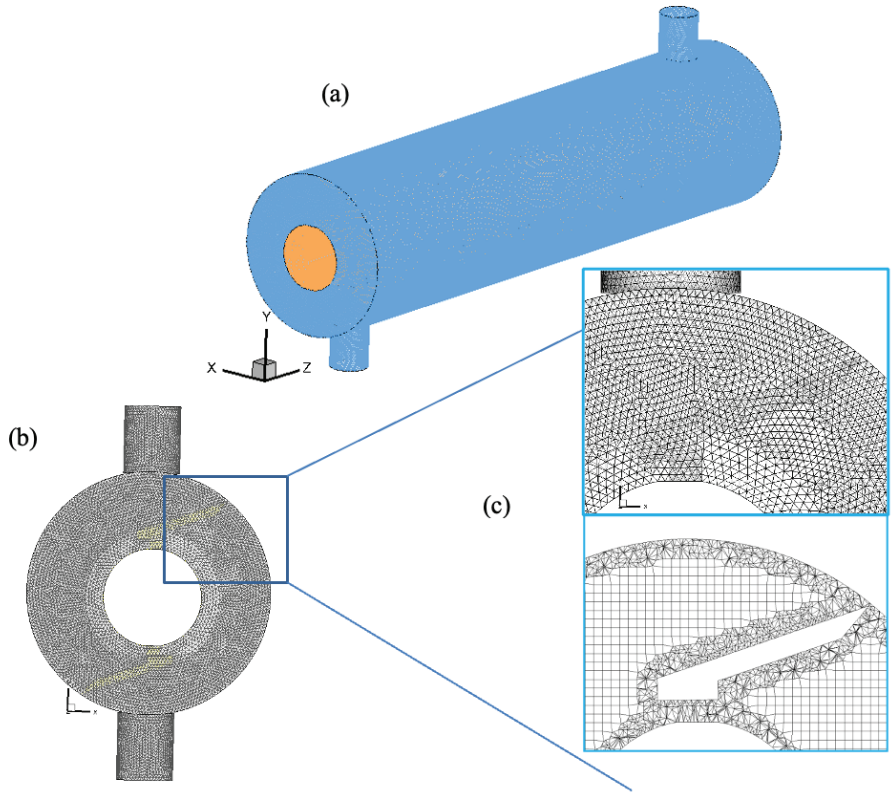

Figure 5. (a) Isometric view of computational mesh of SSHE; (b) Mesh of cross section in SSHE; (c) Enlarged view of the mesh near the clearance between the blade and stator in SSHE.

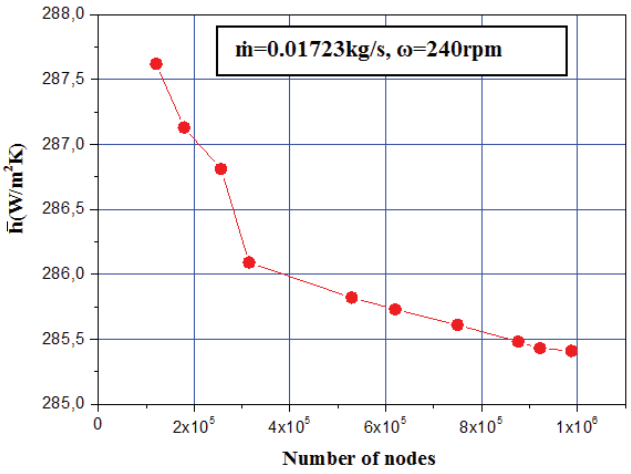

Figure 6. Variation of average convective heat transfer coefficient as a function of the number of nodes for ṁ = 0.017236 Kg/s and ω = 240 rpm.

precision pressure-based solver, a second-order upwind discretization scheme for momentum and energy equations, and the usual scheme for the pressure correction equation. When the normalized residual values for the momentum and mass equations approach 10-3 and the energy equations reach 10-6, respectively, convergence is considered satisfactory [35].

Validation of SSHE Models

In order to verify the accuracy of our simulation results, we calculate the convective heat transfer coefficient and compare it with the numerical data provided by Yataghene and Legrand [13] under identical dimensions and design

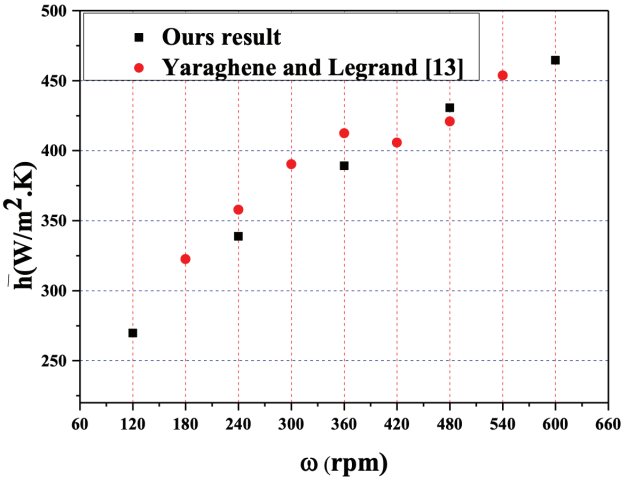

Figure 7. Variation of average convective heat transfer coefficient as a function of rotational speed: A comparison between our results and literature data.

conditions. As illustrated in Figure 7, the comparison demonstrates a favorable agreement, with a maximum deviation of less than 5% evident. This indicates that the methodology adopted in our numerical investigation is viable, and the obtained results can be considered reliable.

RESULTS AND DISCUSSION

This study delves into the impact of several critical factors on the thermal-fluid fields in a specific type of scraped surface heat exchanger (SSHE). Utilizing numerical simulations, the investigation aims to shed light on how these factors influence the performance and efficiency of the SSHE. Mass flow rate ṁ values are considered, which ranged from 0.017 kg/s to 0.086 kg/s. The SSHE with 02, 03 and 04 blades are examined in cases of rotational speed values ω= 120–600 rpm.

Temperature Field and Flow Characteristics in SSHE

The numerical results of the temperature contours are illustrated in Figures 8 to 13 via cross-sections within the scraped surface heat exchanger with 2, 3 and 4 blades for two rotation speeds ω=120 rpm and 600 rpm and for a mass flow rate ṁ =0,051584kg/s, and in different z-locations are

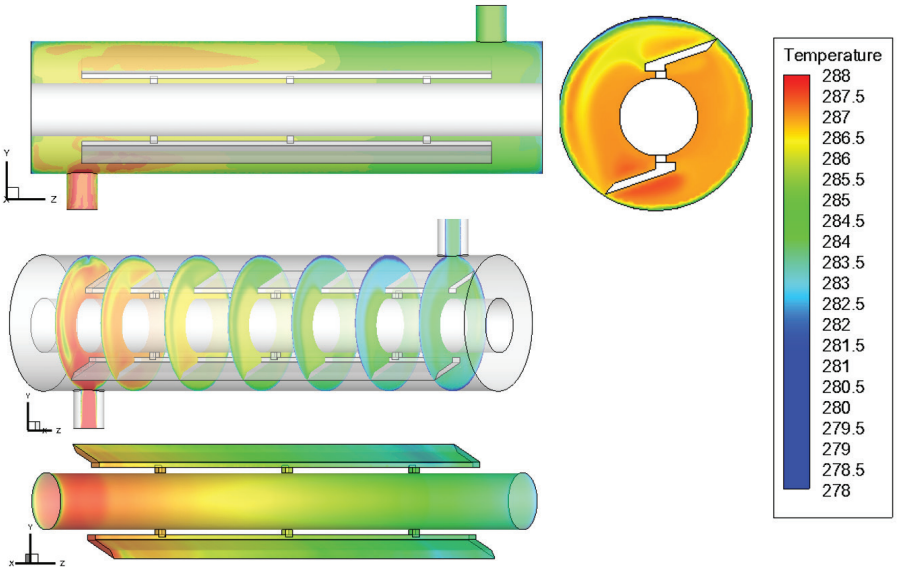

Figure 8. Temperature contour of SSHE with 2 blades in case of ω=120 rpm and ṁ = 0,051584 kg/s.

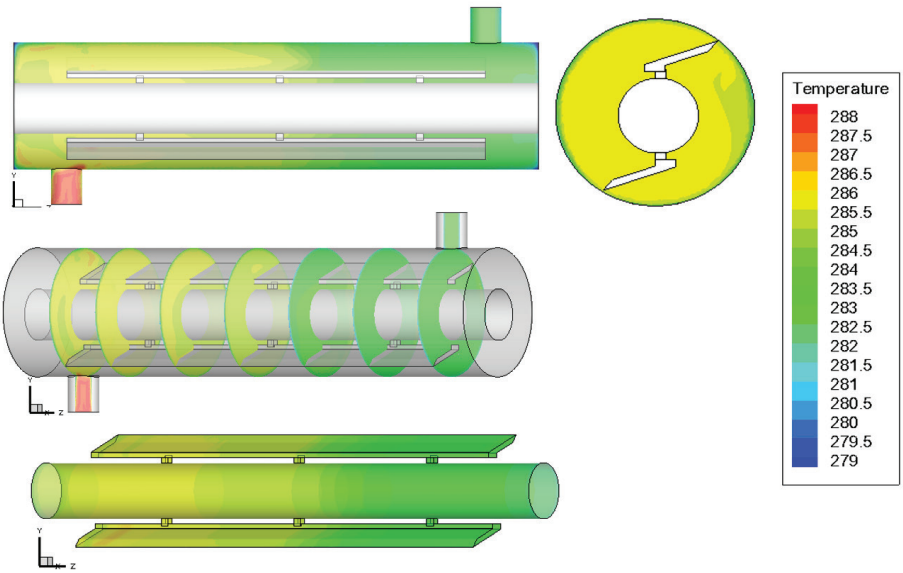

Figure 9. Temperature contour of SSHE with 2 blades in case of ω=600rpm and ṁ = 0,051584 kg/s.

for cross-sections . It is noticed that the fluid enters the heat exchanger cylinder with a temperature of 288.16 K and then gradually decreases In the axial direction, from the inlet towards the outlet, contacting the cold internal surface (278.16 K) of the cylinder. It is clear that in the last part, close to the exit of SSHE, the temperature has not reached the necessary cooling wall temperature, and the fluid leaves at higher temperatures than the cooled wall.

The temperature is not uniformly distributed throughout the heat exchanger, with a more significant temperature difference observed around the blades. This is due to the high shear gradients in these areas. The fluid temperature also decreases with an increase in the number of blades, rotation speed, and mass flow rate. These figures illustrate the development of thermal boundary layers around the blades. A comparison between the 2, 3, and 4-blade exchangers reveals that the thermal boundary layers of the 2-blade exchanger are thinner than those of the 3- and 4-blade exchangers. This is due to the reduction in fluid velocity near the blade surfaces reducing the heat exchange.

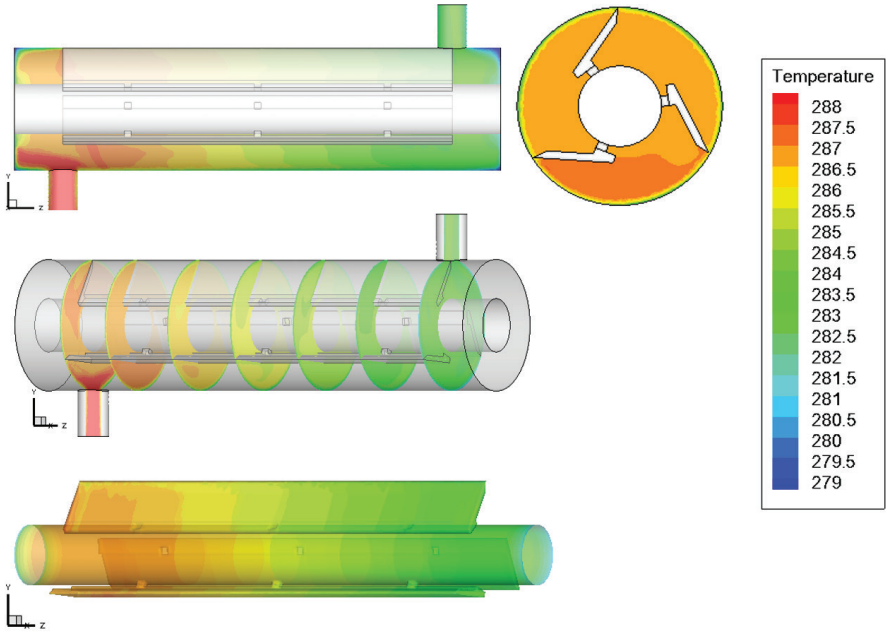

Figure 10. Temperature contour of SSHE with 3 blades in case of ω=120 rpm and ṁ = 0,051584 kg/s.

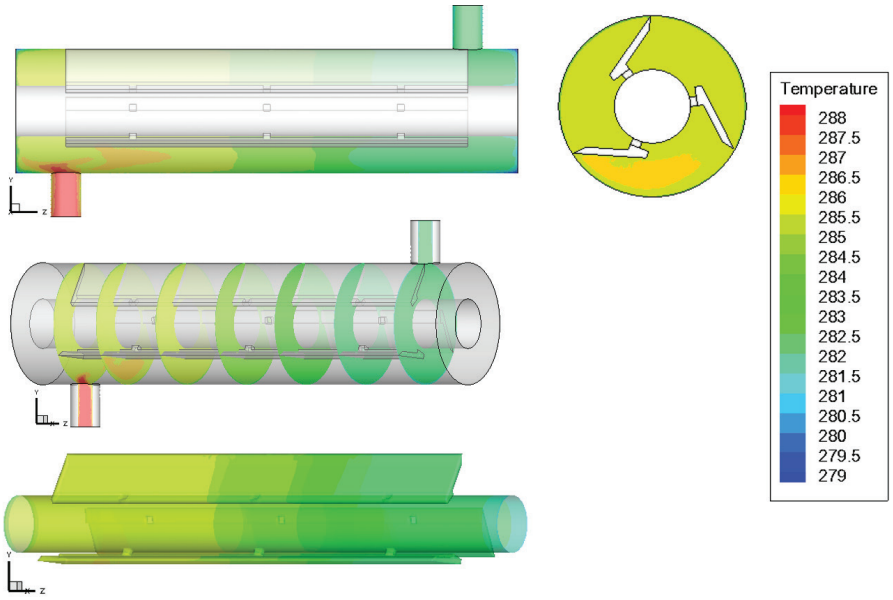

Figure 11. Temperature contour of SSHE with 3 blades in case of ω=600 rpm and ṁ = 0,051584 kg/s.

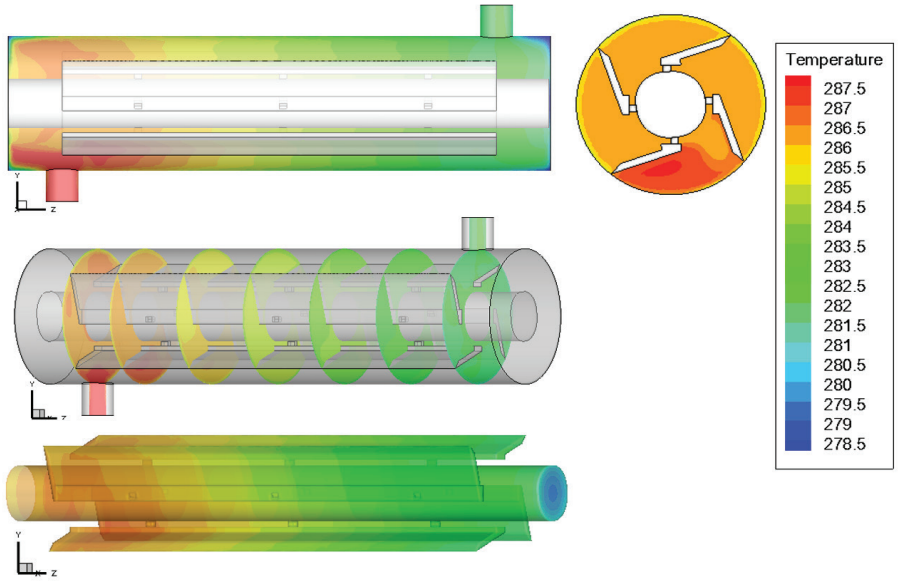

Figure 12. Temperature contour of SSHE with 4 blades in case of ω=120 rpm and ṁ = 0,051584 kg/s.

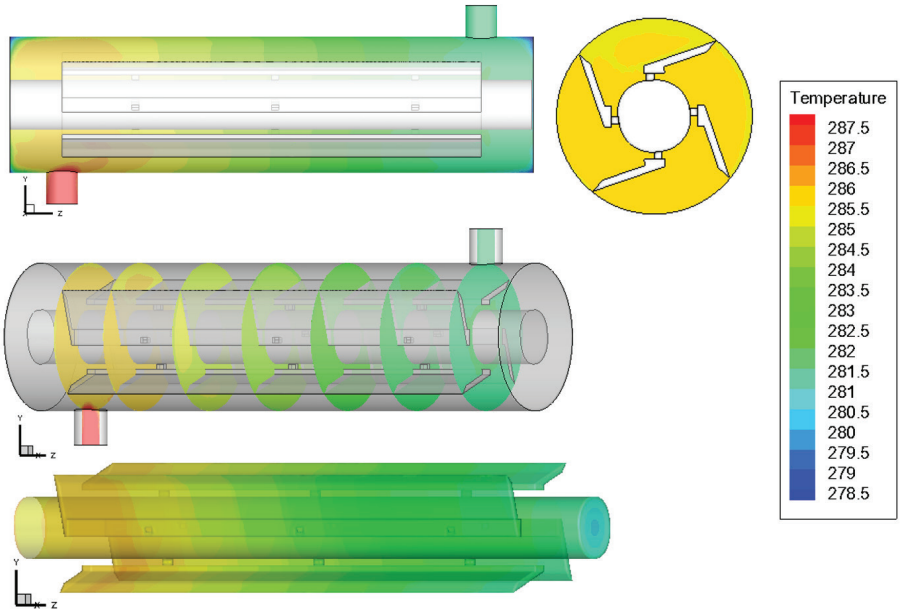

Figure 13. Temperature contour of SSHE with 4 blades in case of ω=600 rpm and ṁ = 0,051584 kg/s.

The Flow Streamlines

Figure 14 & 15 indicate the flow streamlines in the SSHE with two and four blades at rotational speeds ω of 120 rpm and 600 rpm and a mass flow rate ṁ of 0.035 kg/s, revealing significant insights into the fluid motion and heat transfer behavior. The rotational motion of the blades generates vortices on both sides of each blade, with larger vortices forming at the front of the blades due to the rotational forces and smaller vortices observed near the blade tips. These vortices enhance fluid mixing and disrupt the thermal boundary layer, facilitating improved heat transfer. The comparison between two and four-blade configurations indicates that the four-blade setup achieves higher fluid velocities due to increased disturbances and mixing, leading to enhanced convective heat transfer efficiency. At higher rotational speeds, such as 600 rpm, the vortices and fluid velocity intensify further, increasing the interaction between the blades and fluid and minimizing stagnant zones. This thorough mixing ensures consistent thermal exchange by continuously bringing cooler fluid into contact with the heat transfer surface. The findings highlight the critical role of vortex dynamics in optimizing SSHE

performance, with the four-blade configuration demonstrating superior thermal efficiency due to its ability to promote higher fluid velocities and better mixing.

Effect of the Number of The Blades and Rotational Speed

Figures 16 and 17 present the variation of the difference temperature ΔT and Tout as a function of the rotational speed obtained with two, three, and four blades in the case of ṁ = 0.05158 Kg/s

It can be observed that the increase of the number of blades (from two to four) in a scraped surface heat exchanger (SSHE) significantly enhances the heat transfer rate due to improved interaction between the cooling fluid and the exchanger walls. The additional blades increase the surface area of thermal convection, allowing more heat to transfer from the fluid to the walls. Moreover, the blades disrupt the thermal boundary layer more effectively, reducing resistance to heat transfer and facilitating greater convective heat exchange. The enhanced fluid agitation caused by the increased blade count also promotes better mixing, reducing temperature gradients within the fluid and ensuring cooler fluid is continuously brought into contact with the heat transfer surface. As a result, the outlet temperature (Tout) of the fluid decreases, reflecting the efficient removal of thermal energy. Simultaneously, the temperature difference (ΔT=To−Tout) grows, indicating improved cooling efficiency. The four-blade configuration, in particular, achieves superior thermal performance by effectively balancing enhanced heat transfer with fluid flow dynamics, making it more efficient than the two- and three-blade configurations. These results highlight the importance of optimizing blade count to maximize the cooling or heating capabilities of SSHEs in industrial applications.

As the rotational speed ω of a scraped surface heat exchanger (SSHE) increases, the outlet temperature Tout of the fluid decreases, indicating improved heat transfer efficiency. This improvement is primarily due to enhanced fluid mixing and increased interaction with the heat transfer surface at higher speeds. The faster rotation generates more turbulence and agitation within the fluid, disrupting

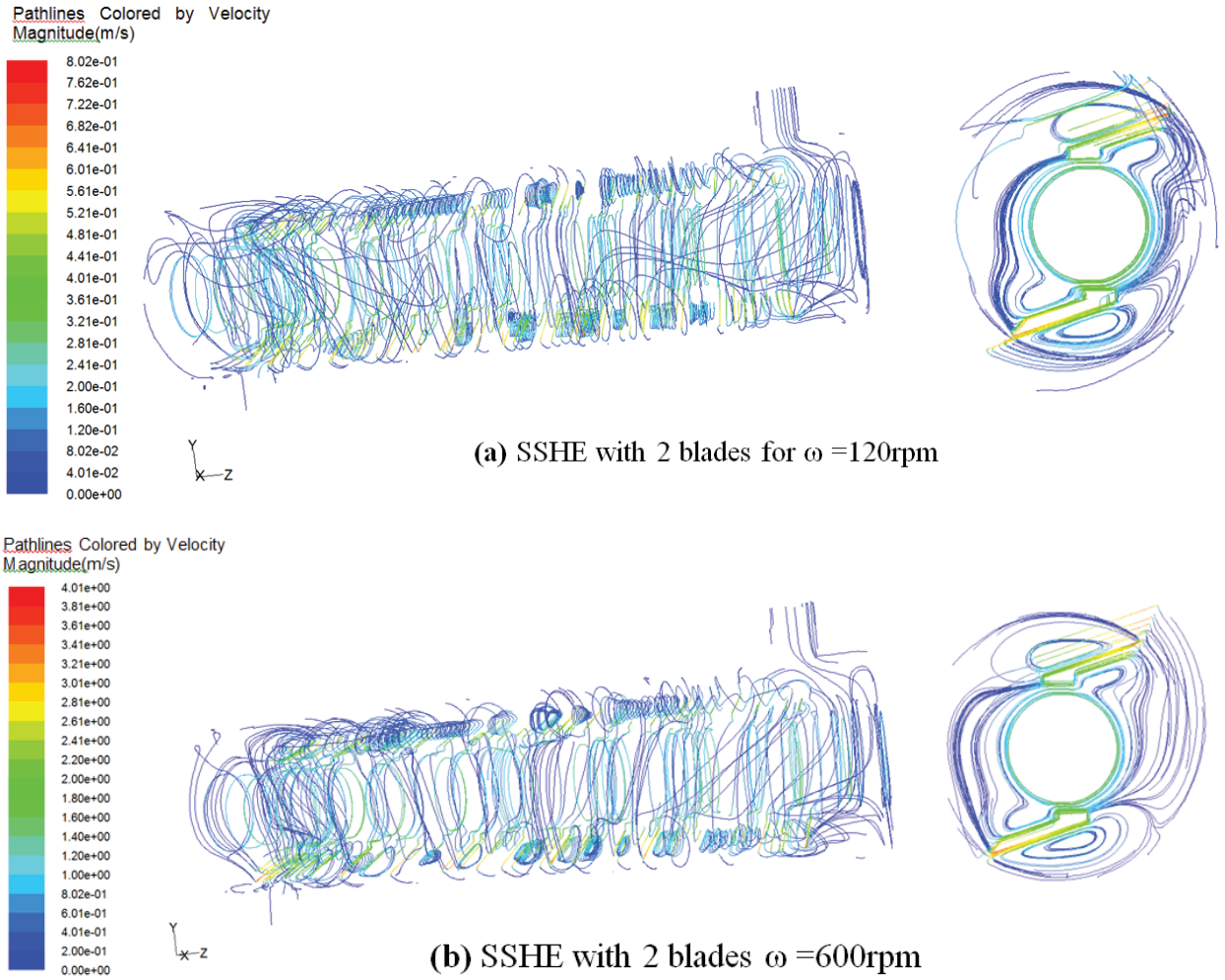

Figure 14. Pathlines in SSHE with two blades for ṁ = 0,035 kg/s and different rotational speed.

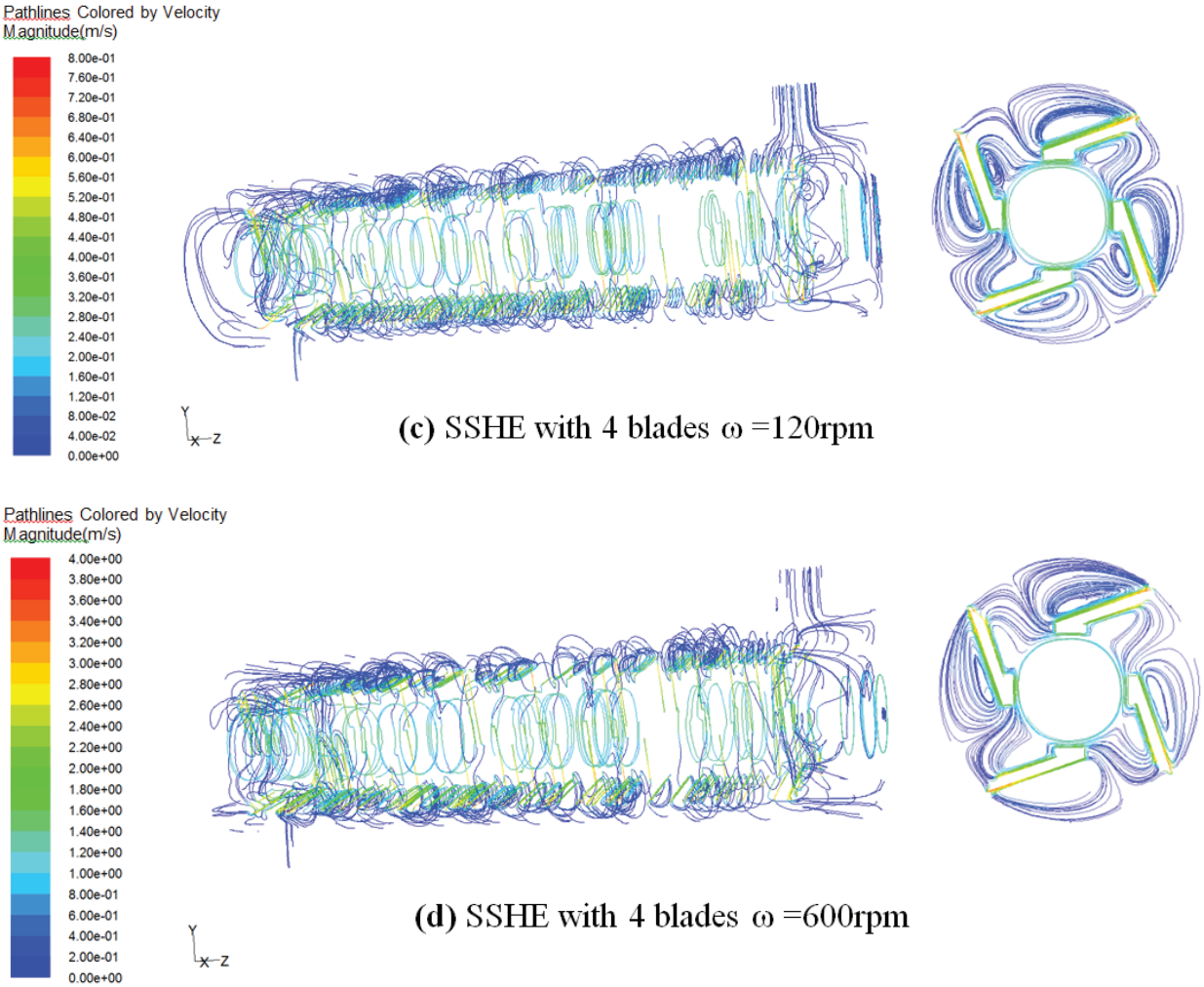

Figure 15. Pathlines in SSHE with four blades for ṁ = 0,035 kg/s and different rotational speed.

stagnant zones and ensuring uniform temperature distribution. Additionally, the increased velocity of the fluid near the blade walls reduces the thickness of the thermal boundary layer, lowering resistance to heat transfer and facilitating more efficient thermal energy exchange. Higher rotational speeds also produce stronger shear forces, which prevent fouling or sedimentation on the exchanger walls, further maintaining optimal heat transfer conditions. Moreover, the elevated rotational speed increases the mass flow rate of the fluid, reducing its residence time in the exchanger. However, this is offset by the enhanced convective heat transfer, ensuring that the overall thermal performance is significantly improved. These combined effects make higher rotational speeds a critical factor for optimizing SSHE efficiency, although careful consideration must be given to energy consumption and mechanical stress to maintain operational sustainability.

The effect of the number of scraper blades and rotational speed ω on the Nusselt number and its percentage enhancement are depicted in Figure 18. The results show that the Nusselt number increases significantly with the rotational speed ω of the SSHE. This increase is attributed to the enhanced velocity of the fluid flow, which intensifies shear forces and disrupts the thermal boundary layer near the heat transfer surface, thereby improving the convective heat transfer coefficient. However, as observed in the percentage improvements, the Nusselt number enhancement diminishes at higher rotational speeds. For instance, with four blades, the maximum enhancement (between SSHE with 4 and 2 blades) is 44.74% at 240 rpm, decreasing slightly to 43.78% at 360 rpm and further to 30.6% at 600 rpm. This reduction in improvement at higher speeds likely reflects diminishing returns as the system approaches its physical limits of convective heat transfer efficiency. The presence of four blades further enhances Nu by increasing the interaction between the fluid and the heat transfer surface, with the greatest impact observed at moderate speeds such as 240 rpm, where fluid mixing and energy input achieve an optimal balance. These findings emphasize the

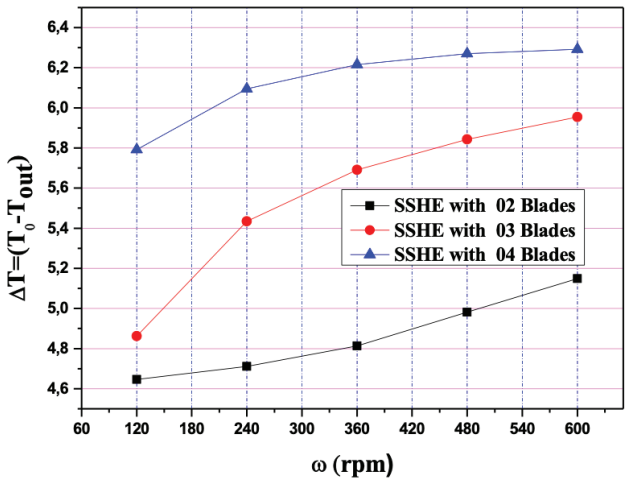

Figure 16. Variation of the difference temperature ΔT as a function of the number of the blades and the rotational speed for ṁ = 0.05158 Kg/s.

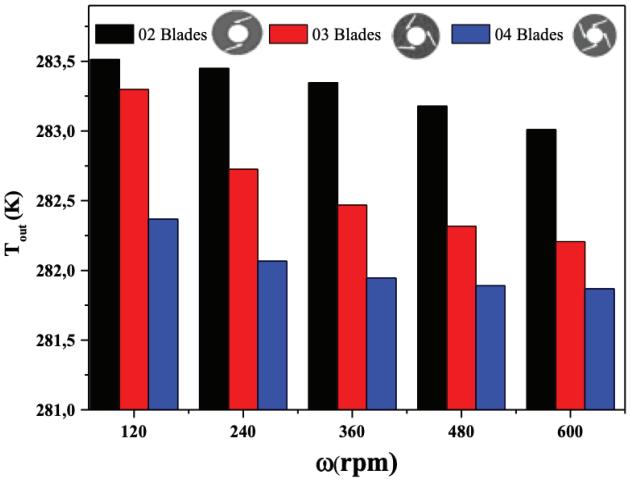

Figure 17. Variation of the temperature T_{out} as a function of the number of the blades and the rotational speed for ṁ = 0.05158 Kg/s.

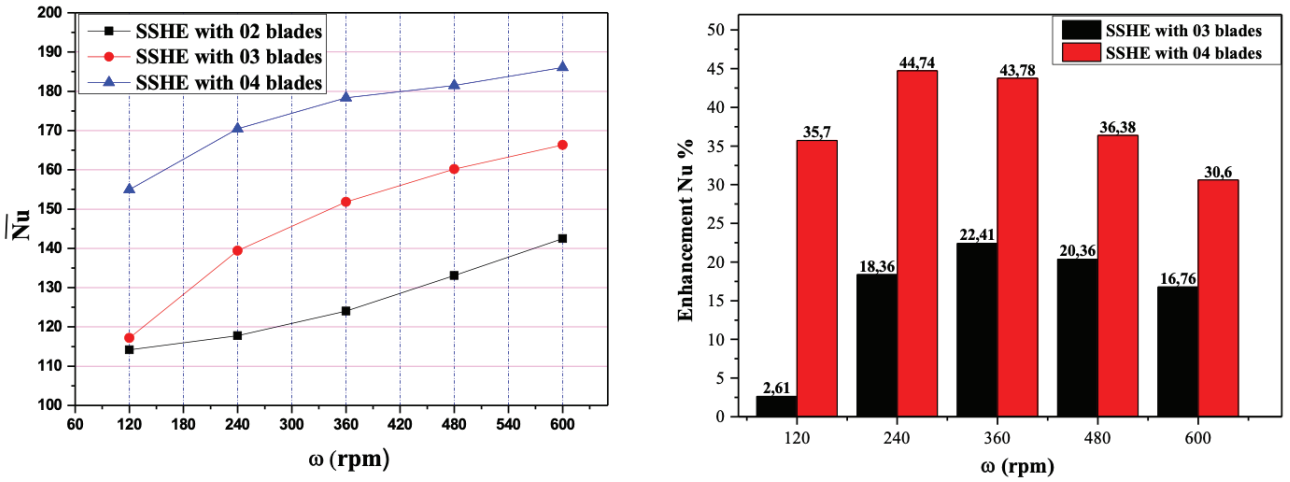

Figure 18. Variation of the average Nusselt number and its enhancement as a function of the rotational speed and the number of the blades for ṁ = 0.05158 Kg/s.

importance of optimizing rotational speed and blade count to maximize the heat transfer efficiency of SSHEs.

Effect of the Inlet Flow Rate

The inlet flow rate significantly influences the thermal performance of a scraped surface heat exchanger (SSHE). As illustrated in Figures 19 and 20, increasing the inlet flow rate results in a sharp decrease in the temperature difference ΔT between the inlet and outlet. This reduction is primarily due to the shorter residence time of the fluid within the SSHE, which limits the duration of thermal interaction with the heat transfer surface. Although higher flow rates enhance fluid velocity and turbulence, promoting better mixing and disrupting the thermal boundary layer, these advantages are counteracted by the reduced residence and mixing times.

For the Nusselt number, the relationship is more complex. At higher inlet flow rates, the fluid velocity increases, leading to enhanced turbulence and disruption of the thermal boundary layer, this promotes convective mixing and increases the heat transfer coefficient locally, resulting in an initial rise in the Nusselt number. However, as the flow rate continues to increase, the reduced residence time and diminished mixing opportunities within the SSHE offset these benefits. The fluid has less time to exchange heat with the walls, which decreases the overall heat transfer efficiency and causes the Nusselt number to plateau or even decline at very high flow rates.

Furthermore, the diminished mixing time due to higher flow rates reduces the effectiveness of the scraping blades, as the fluid moves too quickly to be adequately agitated by the blades. This further limits the disruption of the thermal boundary layer and the enhancement of convective heat transfer, which are crucial for improving Nu. Therefore, while higher flow rates initially lead to an increase in Nu, the improvement diminishes at higher rates as the balance between turbulence and residence time shifts unfavorably.

In summary, increasing the inlet flow rate enhances fluid velocity and turbulence, which can initially improve the Nusselt number. However, the reduced residence time and limited mixing at higher flow rates negatively impact the overall convective heat transfer efficiency. This highlights the need to optimize the inlet flow rate to maintain an effective balance between turbulence, residence time, and thermal interaction for maximising the Nusselt number and overall SSHE performance.

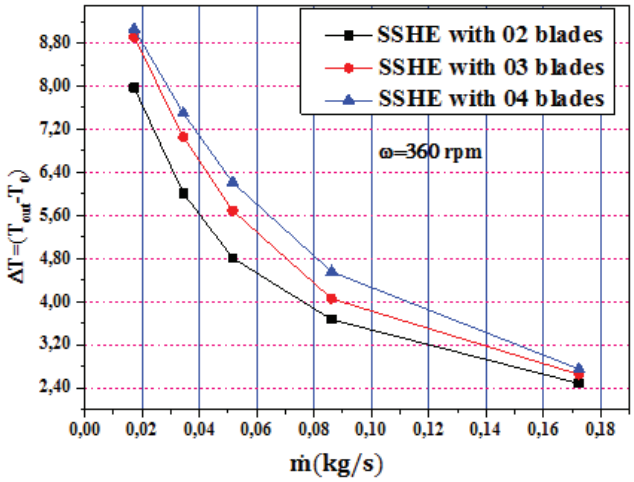

Figure 19. Variation of the difference temperature ΔT as a function of mass flow inlet ṁ and the number of the blades.

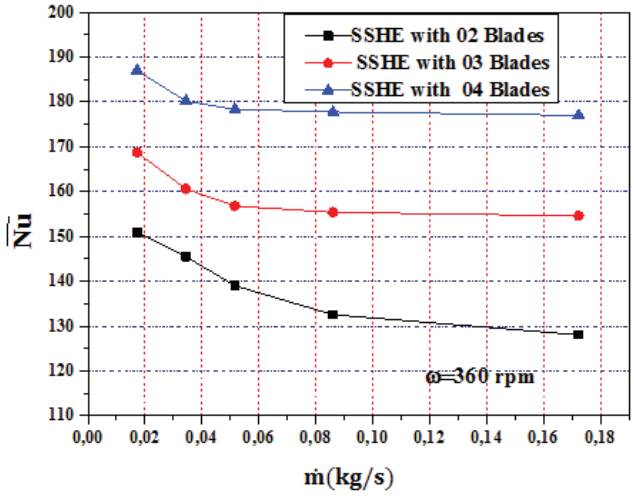

Figure 20. Variation of the average Nusselt number as a function of mass flow inlet ṁ and the number of the blades.

CONCLUSION

This study presented a detailed numerical analysis of the thermal and fluid dynamics performance of a Scraped Surface Heat Exchanger. The investigation focused on key parameters, including the number of blades, rotor speed, and mass flow rate, to optimize heat transfer efficiency and outlet temperature.

The primary findings are as follows:

- The non-uniform temperature distribution was observed, with enhanced cooling near the blades and the heat transfer surface. The thermal boundary layers were thinner in exchangers with fewer blades, which can reduce heat transfer efficiency.
- Increasing the number of blades improves heat transfer by enhancing fluid agitation and increasing the surface area available for convection. The four-blade configuration outperformed the two- and three-blade models in cooling efficiency.
- Higher rotor speeds improved convective heat transfer by boosting fluid velocity and reducing thermal resistance. However, excessively high speeds may require more energy input and should be balanced with system design limitations.
- The impact of mass flow rates on thermal performance was observed: higher flow rates enhance heat transfer but at the cost of increased outlet temperatures due to reduced residence time in the exchanger.
- The Nusselt number increases significantly with rotational speed, driven by intensified fluid velocity and shear forces that enhance convective heat transfer.
- The four-blade configuration delivers the highest Nu, with the greatest percentage improvement observed at moderate speeds (e.g., 44.74% at 240 rpm compared to the two-blade configuration).
- Moderate rotational speeds, such as 240 rpm, offer the best performance in terms of heat transfer efficiency, as they balance fluid mixing and energy input effectively.

Beyond the numerical insights, these findings have significant real-world implications for industries handling high-viscosity fluids, such as food processing, pharmaceuticals, and chemical engineering. The optimization strategies identified in this study can be leveraged to enhance industrial SSHE efficiency, reduce energy consumption, and minimize operational costs. However, real-world applications may introduce additional challenges, such as mechanical wear, energy demands, and hygiene requirements in regulated industries. Future research should explore advanced materials for enhanced durability, adaptive control systems to balance energy efficiency, and real-time monitoring. Additionally, investigating the performance of SSHEs with non-Newtonian fluids and alternative blade geometries can further refine their industrial applicability.

By bridging the gap between numerical modeling and industrial implementation, this study provides valuable insights that can guide engineers, manufacturers, and researchexrs in designing more efficient and sustainable SSHE systems. The integration of computational simulations with experimental validation will be essential for translating these findings into practical, real-world solutions that improve heat exchanger performance in large-scale applications.

NOMENCLATURE

A	Heat transfer area, m^2
d	Hydraulic diameter, m
D_s	Stator diameter, m
D_r	Rotor diameter, m
e	Blade thickness, m
E_r	Relative internal energy, J
H_r	Relative total enthalpy, J
$\overline{h}$	Average heat transfer coefficient, $W/m^2.K$
k_f	Fluid thermal conductivity, W/m.K
L	Stator length, m
$\dot{m}$	Mass flow rate of the fluid, kg/s
$\overline{Nu}$	Average Nusselt number
P	Pressure of the fluid, Pa
q	Heat flux, W
q_c	Convective heat flux, W
$\vec{r}$	Position vector in rotating frame, m
S_{ex}	Total surface heat exchange, m^2
T_0	Inlet temperature of the fluid, K
$\overline{T}_m$	Average temperature of the fluid, K
$\overline{T}_w$	Average temperature of the walls of the SSHE, K
$\vec{V}$	Absolute velocity, m/s
$\vec{v}_r$	Relative velocity, m/s
V_t	Total volume, m^3

Greek Symbols

δ	Blade-stator clearance, μm
μ	Dynamic viscosity, Pa.s
ρ	Density of air, kg/m^3
ω	Rotational speed, rpm

AUTHORSHIP CONTRIBUTIONS

Authors equally contributed to this work.

DATA AVAILABILITY STATEMENT

The authors confirm that the data that supports the findings of this study are available within the article. Raw data that support the finding of this study are available from the corresponding author, upon reasonable request.

CONFLICT OF INTEREST

The author declared no potential conflicts of interest with respect to the research, authorship, and/or publication of this article.

ETHICS

There are no ethical issues with the publication of this manuscript.

STATEMENT ON THE USE OF ARTIFICIAL INTELLIGENCE

Artificial intelligence was not used in the preparation of the article.

REFERENCES

[1] Huggins FE. Effect of scrapers on heating, cooling, and mixing. Ind Eng Chem 1931;23(7):749–53. [CrossRef]

[2] Trommelen A, Beek W. Flow phenomena in a scraped-surface heat exchanger («Votator»-type). Chem Eng Sci 1971;26(12):1933–42. [CrossRef]

[3] Harrod M. Scraped surface heat exchangers: A literature survey of flow patterns, mixing effects, residence time distribution, heat transfer, and power requirements. J Food Process Eng 1986;9:1–62. [CrossRef]

[4] Lee JH, Singh RK. Residence time distribution characteristics of particle flow in a vertical scraped surface heat exchanger. J Food Eng 1993;18:413–24. [CrossRef]

[5] De Goede R, De Jong EJ. Heat transfer properties of a scraped-surface heat exchanger in the turbulent flow regime. Chem Eng Sci 1993;48(8):1393–404. [CrossRef]

[6] Cenedese A, Doglia G, Romano GP, De Michele G, Tanzini G. LDA and PIV velocity measurements in free jets. Exp Therm Fluid Sci 1994;2(9):125–34. [CrossRef]

[7] Baccar M, Abid MS. Numerical analysis of three-dimensional flow and thermal behaviour in a scraped-surface heat exchanger. Rev Gén Therm 1997;36:782–90. [CrossRef]

[8] Alhamdan A, Sastry S. Residence time distribution of food and simulated particles in a holding tube. J Food Eng 1997;34:271–92. [CrossRef]

[9] Alhamdan A, Sastry SK. Residence time distribution of food and simulated particles in a model horizontal swept surface heat exchanger. J Food Process Eng 1998;21:145–80. [CrossRef]

[10] Baccar M, Abid MS. Numerical simulations of hydrodynamic and thermal behaviours in a scraped surface heat exchanger operating in turbulent regime. Int J Therm Sci 1999;38(7):634–44.

[11] Lakhdar MB, Cerecero R, Alvarez G, Guilpart J, Flick D, Lallemand A. Heat transfer with freezing in a scraped surface heat exchanger. Appl Therm Eng 2005;25:45–60. [CrossRef]

[12] Yataghene M, Francine F, Jack L. Flow patterns analysis using experimental PIV technique inside scraped surface heat exchanger in continuous flow condition. Appl Therm Eng 2011;31:2855–68. [CrossRef]

[13] Yataghene M, Legrand J. A 3D-CFD model thermal analysis within a scraped surface heat exchanger. Comput Fluids 2013;71:380–99. [CrossRef]
[14] Martínez DS, Solano JP, Illán F, Viedma A. Analysis of heat transfer phenomena during ice slurry production in scraped surface plate heat exchangers. Int J Refrig 2014;48:221–32. [CrossRef]
[15] Dehkordi KS, Fazilati MA, Hajatzadeh A. Surface scraped heat exchanger for cooling Newtonian fluids and enhancing its heat transfer characteristics: A review and a numerical approach. Appl Therm Eng 2015;87:56–65. [CrossRef]
[16] Błasiak P, Pietrowicz S. An experimental study on the heat transfer performance in a batch scraped surface heat exchanger under a turbulent flow regime. Int J Heat Mass Transf 2017;107:379–90. [CrossRef]
[17] Martínez DS, Illán F, Solano JP, Viedma A. Embedded thermocouple wall temperature measurement technique for scraped surface heat exchangers. Appl Therm Eng 2017;114:793–801. [CrossRef]
[18] Martínez DS, Solano JP, Vicente PG, Viedma A. Flow pattern analysis in a rotating scraped surface plate heat exchanger. Appl Therm Eng 2019;160:113795. [CrossRef]
[19] Pordanjani AH, Vahedi SM, Aghakhani S, Afrand M, Mahian O, Wang LP. Multivariate optimization and sensitivity analyses of relevant parameters on efficiency of scraped surface heat exchanger. Appl Therm Eng 2020;178:115445. [CrossRef]
[20] Maruoka N, Tsutsumi T, Ito A, Hayasaka M, Nogami H. Heat release characteristics of a latent heat storage heat exchanger by scraping the solidified phase change material layer. Energy 2020;205:118055. [CrossRef]
[21] Acosta CA, Yanes D, Bhalla A, Guo R, Finol EA, Frank JI. Numerical and experimental study of the glass-transition temperature of a non-Newtonian fluid in a dynamic scraped surface heat exchanger. Int J Heat Mass Transf 2020;152:119525. [CrossRef]
[22] Tombrink J, Bauer D. Simulation of a rotating drum heat exchanger for latent heat storage using a quasistationary analytical approach and a numerical transient finite difference scheme. Appl Therm Eng 2021;194:117029. [CrossRef]
[23] Tombrink J, Jockenhöfer H, Bauer D. Experimental investigation of a rotating drum heat exchanger for latent heat storage. Appl Therm Eng 2021;183:116221. [CrossRef]
[24] Ding Z, Qin FGF, Peng K, Yuan J, Huang S, Jiang R, Shao Y. Heat and mass transfer of scraped surface heat exchanger used for suspension freeze concentration. J Food Eng 2021;288:110141. [CrossRef]
[25] Egea A, García A, Herrero-Martín R, Pérez-García J. Experimental performance of a novel scraped surface heat exchanger for latent energy storage for domestic hot water generation. Renew Energy 2022;193:870–8. [CrossRef]
[26] Solano JP, Martínez DS, Vicente PG, Viedma A. Enhanced thermal-hydraulic performance in tubes of reciprocating scraped surface heat exchangers. Appl Therm Eng 2023;220:119667. [CrossRef]
[27] Imran A, Shoaib M, Nisar KS, Raja MAZ, Zahra A, Sabir Z. Electroosmosis oriented flow of Jeffrey viscoelastic model through scraped surface heat exchanger. Case Stud Therm Eng 2023;47:103031. [CrossRef]
[28] Egea A, García A, Pérez-García J, Herrero-Martín R. Parametric study of a scraped surface heat exchanger for latent energy storage for domestic hot water generation. Appl Therm Eng 2024;248(Part A):123214. [CrossRef]
[29] Allehiany FM, Imran A, Alqrni MM, Aljohani MA, Al-Mutairi T, Mahmoud EE. A computational investigation for heat and fluid transport with electro-osmosis phenomenon in a scraped surface heat exchanger. Case Stud Therm Eng 2024;61:104988. [CrossRef]
[30] Rahman MA, Dhiman SK. Thermo-fluid performance of a heat exchanger with a novel perforated flow deflector type conical baffles. J Therm Eng 2024;10:868–79. [CrossRef]
[31] Bakhti FZ, Si-Ameur M. A comparison of mixed convective heat transfer performance of nanofluids cooled heat sink with circular perforated pin fin. Appl Therm Eng 2019;159:113819. [CrossRef]
[32] Mishra S, Panda S, Baithalu R, Baithalu R. Enhanced heat transfer rate on the flow of hybrid nanofluid through a rotating vertical cone: A statistical analysis. Partial Differ Equ Appl 2024;20:100825. [CrossRef]
[33] Bakhti FZ, Si-Ameur M, Zerguine B. Enhancement of the cooling by mixed convection of a CPU using a rotating heat sink: Numerical study. Proc Inst Mech Eng Part E J Process Mech Eng 2024;238(1):144–57. [CrossRef]
[34] Al-Obaidi AR, Alhamid J. Influence of different geometrical dimple configurations on flow behaviour and thermal performance within a 3D circular pipe. J Therm Eng 2024;10:175–87. [CrossRef]
[35] Baithalu R, Mishra SR, Shah NA. Sensitivity analysis of various factors on the micropolar hybrid nanofluid flow with optimized heat transfer rate using response surface methodology: A statistical approach. Phys Fluids 2023;35(10):102016. [CrossRef]